AC

FORSCHUNGSZENTRUM ROSSENDORF FZR

FZR-189
August 1997
Preprint

B. Kämpfer, O.P. Pavlenko, A. Peshier,
M. Hentschel, G. Soff

Thermal open charm signals versus hard initial yields in ultrarelativistic heavy-ion collisions

Herausgeber:
FORSCHUNGSZENTRUM ROSSENDORF
Postfach 51 01 19
D-01314 Dresden
Telefon (0351) 26 00
Telefax (0351) 2 69 04 61

Als Manuscript gedruckt

Thermal open charm signals versus hard initial yields in ultrarelativistic heavy-ion collisions‡

B Kämpfer†, O P Pavlenko¶, A Peshier†, M Hentschel§ and G Soff§

† Research Center Rossendorf, 01314 Dresden, PF 510119, Germany

¶ Institute for Theoretical Physics, 252143 Kiev - 143, Ukraine

§ Institut für Theoretische Physik, TU Dresden, D-01062 Dresden, Germany

Abstract. Exploiting a unique set of parton distribution functions we estimate hard processes for open charm, dilepton and mini-jet production. Assuming rapid thermalization within the mini-jet plasma we follow the evolution (expansion and chemical equilibration) of the parton matter and calculate the energy loss of charm quarks in this environment. A substantial part of charm is expected to thermalize. We try to estimate the thermalized open charm component in the final hadron spectra.

1. Introduction

The charm quark possesses a mass of $m_c \cong 1.5$ GeV which is significantly above the QCD scale $\Lambda_{\rm QCD} \sim \mathcal{O}(200$ MeV). Therefore one might expect that the description of charm production is accessible via perturbative QCD in low orders. Indeed, open charm (i.e., D mesons) spectra in collisions at Tevatron energies are well described in next-to-leading order [1]. Higher order calculations [2, 3, 4, 5] with appropriately tuned charm quark mass yield a very accurate data reproduction. (Hidden charm in $c\bar{c} \to J/\psi$ is quite different [6] due to the softer formation dynamics of the bound states.)

Due to its large mass, charm is not as copiously produced as strangeness. From the low strange quark mass $m_s \sim \Lambda_{\rm QCD}$ one expects that strangeness at midrapidity in hadron or heavy-ion collisions at beam energies of 100 GeV and above behaves similar as the up and down quarks [13]. Therefore the open charm signal can be considered as useful complementary probe of the collision dynamics in heavy-ion reactions. Charm is expected to be produced mainly at very early stages in first-chance collisions of partons [4, 7, 8, 9], while strangeness, due to $m_s \sim T_c$ (here T_c stands for the confinement temperature), can be 'cooked' at later and cooler stages of the deconfined matter. Thus the picture emerges that open charm is a primordial probe which experiences the

‡ Supported by BMBF 06DR666 and GSI.

full time span of the highly excited, strongly interacting matter. Also hadronization, especially due to the capture of a light quark, is believed not to affect the open charm dynamics.

There is a further motivation for the consideration of open charm. As predicted recently [4, 10], the so-called correlated semi-leptonic decay of a $D\bar{D}$ pair (produced in the reaction $c\bar{c} \to D\bar{D}$) due to $D\bar{D} \to lX\bar{l}X'$ constitutes a huge background of dileptons $l\bar{l}$, which even exceeds the dilepton signal from the Drell Yan process by a factor 20 (6) according to [4] ([3]) at invariant mass $M \sim 2$ GeV. If this would be the case, there would be a little chance to find a thermal dilepton signal. As pointed out however by Shuryak [11], in heavy-ion collisions the charm quark experiences quite intense interactions with the environment and, as a result, the initial spectrum is drastically changed. This effect is interesting in itself, since it can serve as a measure of the collective dynamics because it depends on the life time of deconfined matter (and therefore should strongly differ in pp and AA collisions). But its mean appeal comes from the fact that it reduces the relative motion of the c and $\bar{c}$ so that in correlated decays the dileptons with larger invariant mass are strongly suppressed and thus the feasibility for detecting a thermal dilepton signal is enlarged.

In the present contribution we try to calculate on a unique footing the hard initial processes of (i) parton scattering into the midrapidity region, (ii) open charm production, and (iii) dilepton production. From (i) we then estimate possible initial conditions of a thermalized phase which we appropriately model. In such a manner we envisage a complete schematic picture for comparing thermal and hard initial charm and dilepton signals. During the thermal phase we then calculate the energy loss of open charm. We find that a substantial fraction of hard charm is likely to stick in the thermalized medium. Instead of extending the charm dynamics up to hadron freeze-out throughout the confinement [12] we make use of the hypothesis that open charm spectra are similar to all other hadron spectra at midrapidity. On this basis, supported by an analysis of present hadron spectra in Pb + Pb collisions at SPS, we try to predict the thermalized component of the final open charm spectrum at RHIC. This might later serve as starting point for estimating the resulting dilepton spectrum from correlated charm decays.

2. Hard initial processes

If the parton distributions $f(x, Q^2)$ as a function of momentum fraction x and resolution scale Q^2 in nuclei A and A$'$ are given, one can calculate the hard particle production at midrapidity. Within the usual parton approach the scheme looks obviously like

$$dN_3 \sim \sum \int x_1 x_2 \, f_A(x_1, Q^2) \, f_{A'}(x_2, Q^2) \, \hat{\sigma}_{12 \to 3X} \cdots, \tag{1}$$

where the sum runs over all parton species which contribute to the subprocess $1+2 \rightarrow 3+X$ (with $\hat{\sigma}_{12\rightarrow 3X}\cdots$ as corresponding cross section), and the integral goes over the kinematical accessible range (depending on the variables in which the rate dN_3 is differential) and it is supplemented by appropriate δ function with corresponding variables. Examples are mentioned above, e.g., the Drell Yan process (where 3 denotes the lepton pair), or the charm and heavy quark production (3 stands for the heavy quark and its anti-quark), inclusive jets (where 3 is a high-energy parton), and mini-jets (where 3 is again a parton with transverse momentum $p_\perp > p^*$ with $p^* \sim \mathcal{O}(2$ GeV) [13]. The first two processes are described already in lowest order perturbation theory with accuracy of a factor 2 (to be absorbed in appropriate K factors). The last process is not sufficient to account for the observed transverse energy, therefore one has to add a suitably parametrized soft component. (The self-consistent screening [14] avoids such a distinction of soft and hard components.) With a given transverse momentum distribution and number distribution of partons at midrapidity, resulting from equation (1), one can calculate the corresponding energy density [8, 9, 13], and by the assumption of rapid thermalization within such a dense medium [13, 15, 16] one can estimate the temperature (as measure of the transverse momentum scale) and phase space occupation factors $\lambda^{q,g}$ (as measure of the density). Results for the MRS D-' parton distribution functions with appropriate nuclear shadowing are for RHIC $T_i \cong 550$ MeV, $\lambda_i^g \cong 0.5$, $\lambda_i^q \cong \lambda_i^g/5$ at initial proper time $\tau_i \cong 0.2$ fm/c, which would correspond to a final pion rapidity density of $dN_\pi/dy \cong 1100$ [9] in agreement with other estimates [8, 13, 15, 16].

3. Thermalized deconfined matter/Thermal versus hard initial yields

Instead of following the evolution of matter in all details by considering the transverse expansion coupled to longitudinal expansion together with phase space saturation processes by chemical rate equations à la reference [17], we here neglect transverse expansion due to the short time scales and model the chemical saturation by quadratic evolution laws $\lambda^{q,g} \propto \tau^2$ with the requirement that at $T_c = 169$ MeV full saturation is achieved, i.e., $\lambda^{q,g} = 1$. The evolution of the energy density of the parton gas is assumed as $e \propto \tau^{-4/3}$, where $e = (d_g\lambda^g + d_q\lambda^q)T^4$ in accordance with an ideal gas equation of state and with standard degeneracy factors $d_{q,g}$.

On the first glance this is a poor parametrization of deconfined matter. Indeed, it gets some support by an extrapolation of recent lattice data. Figure 1 displays the data (symbols) of the equation of state of 4-flavor QCD in the chiral limit with some finite size corrections [18]. The lines depict the extrapolation of our quasi-particle model [19], where all of the complexity of strong interaction is absorbed in temperature dependent effective gluon and quark masses. A quite perfect description of the data is obviously achieved. Remarkably, the energy density above T_c looks like an ideal gas with $e \propto T^4$,

as assumed above. Figure 2 shows the resulting equation of state for gluons, two light flavors and one strange quark with rest mass. The basic features from Figure 1 are pertinent.

Within such an evolution scenario the thermal dilepton and open charm yields can be compared with the hard initial production in a coherent manner. In particular, using again the HERA supported structure functions MRS D-' we have studied the general tendency of the competition between thermal signals and hard initial yields with respect to the change of the collider energy [9]. The thermal dilepton signal with invariant mass in the so-called continuum region $M \sim 2 - 3$ GeV is found to rise much stronger as compared to the hard Drell Yan background with increasing collider energy and clearly dominate at LHC energy. This is not the case for open charm: even at LHC energy and for a very rapid thermalization, the thermal yield of charm is estimated to much smaller than the initial hard rate.

4. Energy loss of charm quarks

In order to demonstrate the importance of the energy loss effect of charm quarks for the D meson production in heavy-ion collisions, which is needed for estimating the background to a direct dilepton signal, we employ a simplified model wherein charm is initially produced at midrapidity and then propagates from the center of a matter slice. In such a model all calculations become very transparent and can serve as a qualitative hint for more involved Monte Carlo simulations. We adopt here the recent approach of Baier et al. [21, 22] to estimate the energy loss of a fast midrapidity-parton with transverse momentum $p_\perp$ traversing parton matter:

$$\frac{dp_\perp}{d\tau} = -\frac{4}{3}\frac{\alpha_s k_c}{\sqrt{L}}\,(p_\perp^2 + m_c^2)^{1/4}\,\ln\left(\frac{\sqrt{p_\perp^2 + m_c^2}}{L\,k_c^2}\right), \tag{2}$$

$$\frac{dr_\perp}{d\tau} = \frac{p_\perp}{\sqrt{p_\perp^2 + m_c^2}} \tag{3}$$

with $k_c^2 = 2m_{th}^2(T) = \frac{8}{9}(\lambda_g + \frac{1}{2}\lambda_q)\pi\alpha_s T^2$ and $L^{-1} = 2.2\,\alpha_s\,T$. The modifications introduced here are the following ones: We estimate the mean free path in a gluon bath as $L^{-1} \sim \sigma_{gg}\,n_g$ with integrated cross section $\sigma_{gg} \sim \alpha_s^2/k_c^2$ and gluon density $n_g \sim \lambda_g T^3$. Probably the most crucial quantity is the cut-off parameter k_c for regularizing the cross sections. Strictly speaking equations (2, 3) are derived for fast partons; here we employ them for all velocities. While in references [11, 23] an averaged stopping power $dE/dx = -2$ GeV/fm and $L = 1$ fm are assumed, we integrate these equations together with the above described time evolution of $T(\tau)$, $\lambda^{q,g}(\tau)$. Results are displayed in figure 3, where the transverse momentum of a charm quark at confinement temperature, $p_\perp^c$, is shown as a function of its initial momentum, $p_\perp^0$, supposed the charm quark propagates

all the time parton matter. With the above parameters and $\alpha_s = 0.3$ one finds that charm with $p_\perp^0 < 1$ GeV is fully stopped, while for $p_\perp^0 > 1$ GeV the final transverse momentum is diminished to a half of the initial value. This finding is in accordance with other approaches [11, 23] where also an substantial stopping is found.

These charm quarks which are completely stopped will undergo thermal motion and collective transverse flow. From figure 3 one interferes that even for $p_\perp^0 < 2.5$ GeV the final transverse momentum is below the averaged thermal momentum, and also this wider interval could be attributed to the stopped and thermalized component. The final spectrum of momentum-degraded (i.e., non-stopped) charm at midrapidity can be constructed from

$$\frac{dN^c}{d^2p_\perp^c} = \frac{p_\perp^0(p_\perp^c)}{p_\perp^c} \frac{dp_\perp^0(p_\perp^c)}{dp_\perp^c} \frac{dN^0(p_\perp^0)}{d^2p_\perp^0}\bigg|_{p_\perp^0(p_\perp^c)} . \tag{4}$$

This quantity is displayed in figure 4 together with the initial spectrum [9] (here without shadowing).

We note an interesting observation: When comparing the momentum-degraded spectrum with the thermalized one, we find for $p_\perp < 2$ GeV much similarity. In calculating the thermalized spectrum we employ the parametrization [24]

$$\frac{dN}{d^2p_\perp} \propto \int_0^1 d\xi\, \xi\, m_\perp\, K_1\left(\frac{m_\perp}{T}\mathrm{ch}\rho\right) I_0\left(\frac{p_\perp}{T}\mathrm{sh}\rho\right) \tag{5}$$

(with $m_\perp$ as transverse mass and $\rho = \tanh^{-1}(\frac{2}{3}\xi v_\perp^{\mathrm{aver}})$) for $T = T_c$ and $v_\perp^{\mathrm{aver}} \cong 0.2$ as follows from our hydro code [25, 26] for the given initial conditions. Due to this observation one can expect that a considerable part of charm is expected to look like the other thermalized and transversally flowing matter. Only those charm quarks which have a distance < 2.5 fm (which is the maximum distance traversed up to confinement) to the transverse edge of the system have a chance to escape with much less stopping [23]. These ones will constitute a still hard transverse component in the open charm spectrum and need further investigations to adjust their corresponding weight in the full spectrum.

We mention that there might be further momentum changes due to the effects of a possible mixed phase and the hadronic stage [12]. Instead of considering the poorly known details of the confinement dynamics we focus in the following on that part of open charm which is sufficiently stopped to flow commonly with all other hadrons. From the above considerations we expect that this is a considerable fraction, in contrast to pp collisions, where such a stopping mechanism due to an extended and dense environment is not operative.

5. Hadron spectra

Here we present an argument in favor of our hypothesis that the transverse momentum phase space distribution of all final hadrons at midrapidity in central collisions at high beam energy can be parametrized by a unique freeze-out temperature and a unique transverse flow.

5.1. Hadron spectra at SPS

The presently available transverse momentum spectra at midrapidity in central Pb + Pb collisions at SPS (158 AGeV), measured by the NA49 collaboration [27], can by parametrized by equation (5) with $T = 120$ MeV and $v_\perp^{\rm aver} = 0.43$ [28]; also the very preliminary deuteron data fit in this picture, see Figure 5. In a macroscopic, phenomenological language one can derive equation (5) [24] from the sudden freeze-out of transversely flowing matter with linear velocity profile but constant temperature and chemical potential on proper time surfaces.

We mention that the parametrization of the low-$p_\perp$ pion data from NA44 [29] require a modification of the final phase space distribution by a chemical potential of the corresponding Bose distribution with $\mu_\pi = 135$ MeV in

$$\frac{dN}{d^2p_\perp} \propto \int_0^1 d\xi\, \xi\, m_\perp \sum_{n=1}^{\infty} \exp\left\{\frac{n\mu_\pi}{T}\right\} K_1\left(\frac{nm_\perp}{T}{\rm ch}\rho\right) I_0\left(\frac{np_\perp}{T}{\rm sh}\rho\right). \qquad (6)$$

We stress that equations (5, 6) are considered here as useful parametrization of the final phase space distributions, and we do not intent to describe by an underlying fire ball model at the same time the hadron abundancies and feeding effects by resonance decays. In this spirit the deduced values for T and $v_\perp^{\rm aver}$ are pure parameters of a certain fit function.

Nevertheless, it is remarkable that such a unique description of the hadron spectra is possible. This novel fact is displayed in Figure 6. As well known [30] one can equally well fit a given spectrum of one hadron species by a large range of values of T and $v_\perp^{\rm aver}$ yielding a curve $v_\perp^{\rm aver}(T)$. In contrast to the previous S + S data from SPS, which do not fix the flow without additional requirements [30], the NA49 data for Pb + Pb have a focus of all the individual functions $v_\perp^{\rm aver}(T)$, see Figure 6. The same fact might be quantified by displaying the contour plot of the chi square function $\chi^2(T, v_\perp^{\rm aver}) = \sum_{i=1}^{9} \chi^2_{i,{\rm dof}}$, see Figure 7. One observes the long valley with the shallow minimum at the above mentioned values.

We mention that our hydro code [25, 26] supports the above value of T and $v_\perp^{\rm aver}$ in the following sense. For the initial conditions $\tau_i = 1$ fm/c and temperature $T_i \sim 200$ MeV with a resonance gas equation of state (thus reproducing the experimental charged-pion rapidity density) one can display at each time instant T and $v_\perp$ yielding a line which

crosses the minimum in Figure 7.

5.2. Hadron spectra at RHIC

One line of further investigations is to exploit the above quoted initial conditions suitable for RHIC to extract again with the hydro code values of $T(v_\perp^{\rm aver})$ during the expansion. We find that due to the very large initial pressure, the transverse expansion is strong, and at $T \cong 120$ MeV the values of $v_\perp^{\rm aver}$ approach the limiting number 0.66. It might be that, as a consequence of the rapid expansion, the kinetic freeze-out appears at higher temperatures and lower transverse expansion velocity. Therefore, we conclude that the prediction of hadron spectra at RHIC conditions needs further investigations with dynamical freeze-out criteria. Once one has some reliable estimates of T and $v_\perp^{\rm aver}$ for RHIC one can proceed with the phase space parametrization equation (5) and generate the distribution of D mesons and study the resulting dileptons from their semi-leptonic decays. Work in this direction is in progress.

In conclusion let us remark that the parametrization of the spectra by equation (5) with a unique set of values T and $v_\perp^{\rm aver}$ valid for all hadrons is quite intriguing - although it might be accidental for the Pb + Pb data [27] within their restricted acceptance window. For instance, the transport model RQMD [31] predicts a more complex freeze-out dynamics which is hardly described as sudden and unique freeze-out. But we stress again here that we are interested in phase space parametrizations of the final hadrons and the possibility to have a link to global hydrodynamics [26].

6. Summary

In summary, we find as other authors [11, 23] hints for strong charm stopping in central heavy-ion collisions at RHIC. This effect is experimentally accessible and should show up as pronounced difference to the transverse open charm spectra in pp or pA collisions. Such an energy loss of open charm reduces the large-mass dilepton background from correlated semi-leptonic charm decays and still leaves a possibility for extracting a dilepton excess in the invariant mass region $M \geq 2$ GeV stemming from a thermal source.

[1] McGaughey P L 1996 *Nucl. Phys.* **A 610** 394c
[2] Smith J and Vogt R 1996 *hep-ph* 9609388
[3] Fein D, Huang Z, Valerio P and Sarcevic I 1996 *hep-ph* 9607264
[4] Gavin S, McGaughey P L, Ruuskanen P V and Vogt R 1996 *Phys. Rev.* **C 54** 2606
[5] Sarcevic I and Valerio P 1995 *Phys. Rev.* **C 51** 1433
[6] Sansoni A et al. (CDF) 1996 *Nucl. Phys.* **A 610** 373c

[7] Lin Z and Gyulassy M 1995 *Phys. Rev.* **C 51** 2177
[8] Levai P, Müller B and Wang X N 1995 *Phys. Rev.* **C 51** 3326
[9] Kämpfer B and Pavlenko O P 1997 *Phys. Lett.* **B 391** 185
[10] Vogt R, Jacak B V, McGaughey P L and Ruuskanen P V 1994 *Phys. Rev.* **D 49** 3345
[11] Shuryak E 1997 *Phys. Rev.* **C 55** 961
[12] Svetitsky B and Uziel A 1997 *Phys. Rev.* **D 55** 2616
[13] Eskola K 1995 *Nucl. Phys.* **A 590** 383c
[14] Eskola K J, Müller B and Wang X N 1996 *hep-ph* 9608013, *Phys. Lett.* **B 374** 20
[15] Geiger K 1995 *Phys. Rep.* **258** 237
[16] Wang X N 1997 *Phys. Rep.* **280** 287
[17] Kämpfer B, Pavlenko O P, Peshier A and Soff G 1995 *Phys. Rev.* **C 52** 2704
[18] Engels J, Joswig R, Karsch F, Laerman E, Lütgemeier M and Petersson B 1996 *hep-lat* 9612018
[19] Peshier A, Kämpfer B, Pavlenko O P and Soff G 1996 *Phys. Rev.* **D 54** 2399
[20] Pisarski R D 1989 *Nucl. Phys.* **A 498** 423c
[21] Baier R, Dokshitzer Yu L, Peigne S and Schiff D 1995 *Phys. Lett.* **B 345** 277
[22] Baier R, Dokshitzer Yu L, Mueller A H, Peigne S and Schiff D 1996 *Nucl. Phys.* **B 478** 577
[23] Lin Z, Vogt R and Wang X N 1997 *nucl-th* 9705006
[24] Heinz U, Lee K S and Schnedermann E 1990 *NATO ASI* **B 216** 385
[25] Kämpfer B and Pavlenko O P 1994 *Z. Phys.* **C 62** 491
[26] Hentschel M 1997 *Diploma thesis* TU Dresden
[27] Jones P G et al. (NA49) 1996 *Nucl. Phys.* **A 610** 188c
[28] Kämpfer B 1996 *hep-ph* 9612336
[29] Bearden I G et al. (NA44) 1997 *Phys. Rev. Lett.* **78** 2080
[30] Schnedermann E, Sollfrank J and Heinz U 1993 *Phys. Rev.* **C 48** 2462
[31] Stöcker H 1997 *talk at* Strange Quark Matter, Santorini, Greece

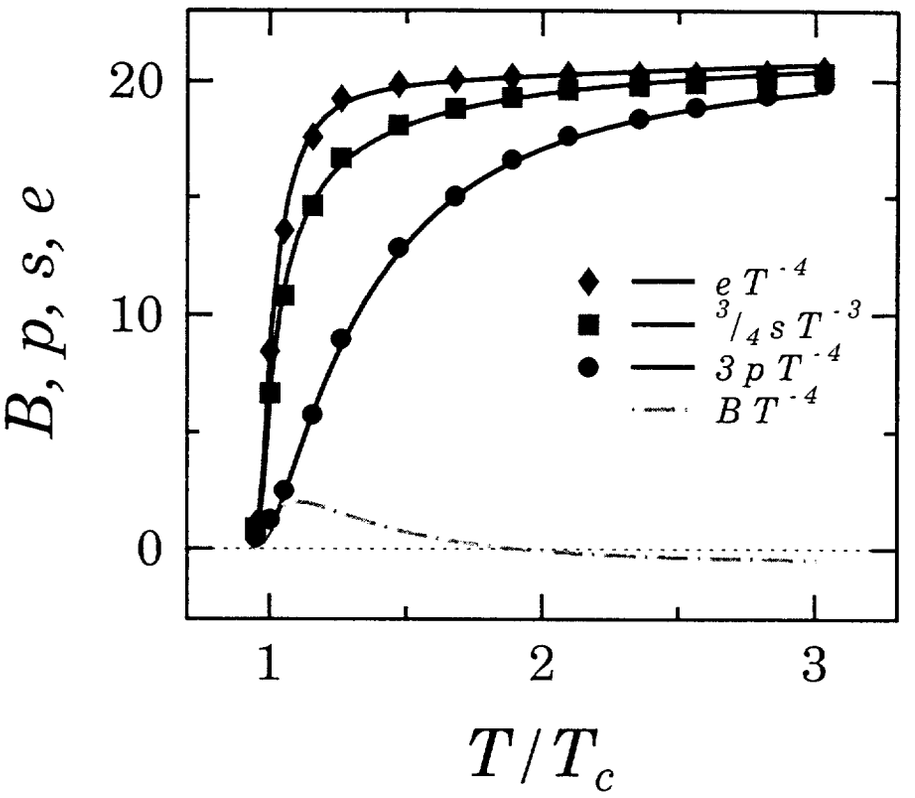

Figure 1. Description of the 4-flavor lattice QCD data [18] (symbols) by our model [19], which rests on the entropy density $s = s_{\rm id}(T, m(T))$, energy density $e = e_{\rm id}(T, m(T)) + B(T)$, pressure $p = p_{\rm id}(T, m(T)) - B(T)$, where the temperature dependent quasi-particle masses $m(T) \propto G(T)\, T$ follow from high-temperature QCD since $\lim_{T\to\infty} G(T) = g(T)$ with $g(T)$ as one-loop running coupling constant. The subscript "id" means the corresponding ideal gas expressions; the function $B(T)$ follows from thermodynamical self-consistency.

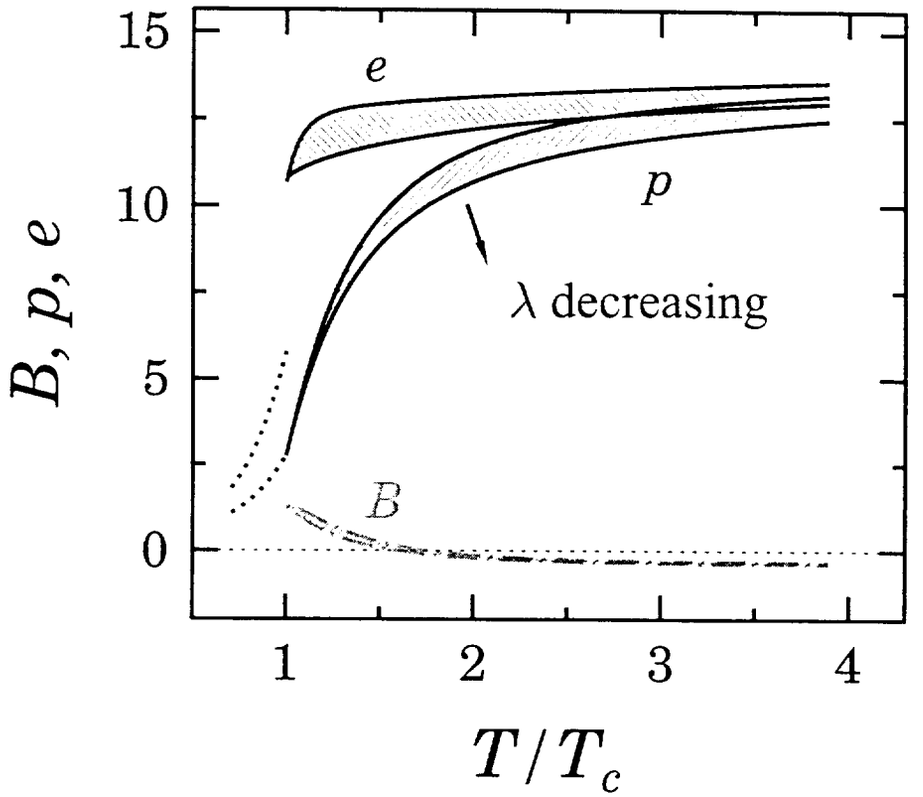

Figure 2. Our prediction of the equation of state (scaled by T^4) of interacting gluons, light u, d quarks and massive strange quarks. The quasi-particle model from Figure 1 is applied but now adjusted to a constructed 1^{st}-order phase transition to a resonance gas at T_c (all resonances up to 2 GeV mass, dotted lines). The temperature dependent strange quark mass becomes here $m_s(T) \to m_s/2 + (m_s^2/2 + m(T)^2)^{1/2}$ according to the hard thermal loop results [20]. λ is an internal model parameter for regularizing the effective coupling parameter.

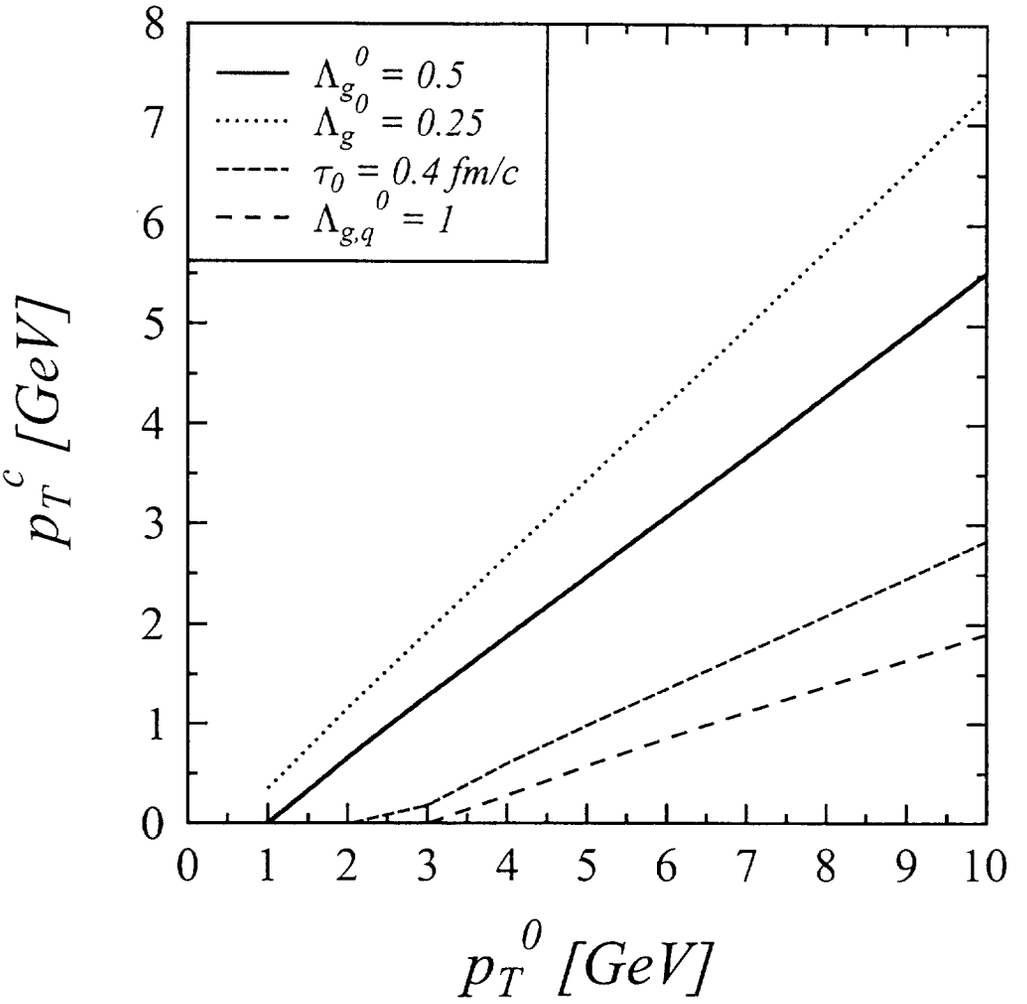

Figure 3. Final transverse momentum vs. initial momentum of charm quarks according to equations (2, 3) for various initial parameters. The full line depicts the results for the initial conditions quoted in the text.

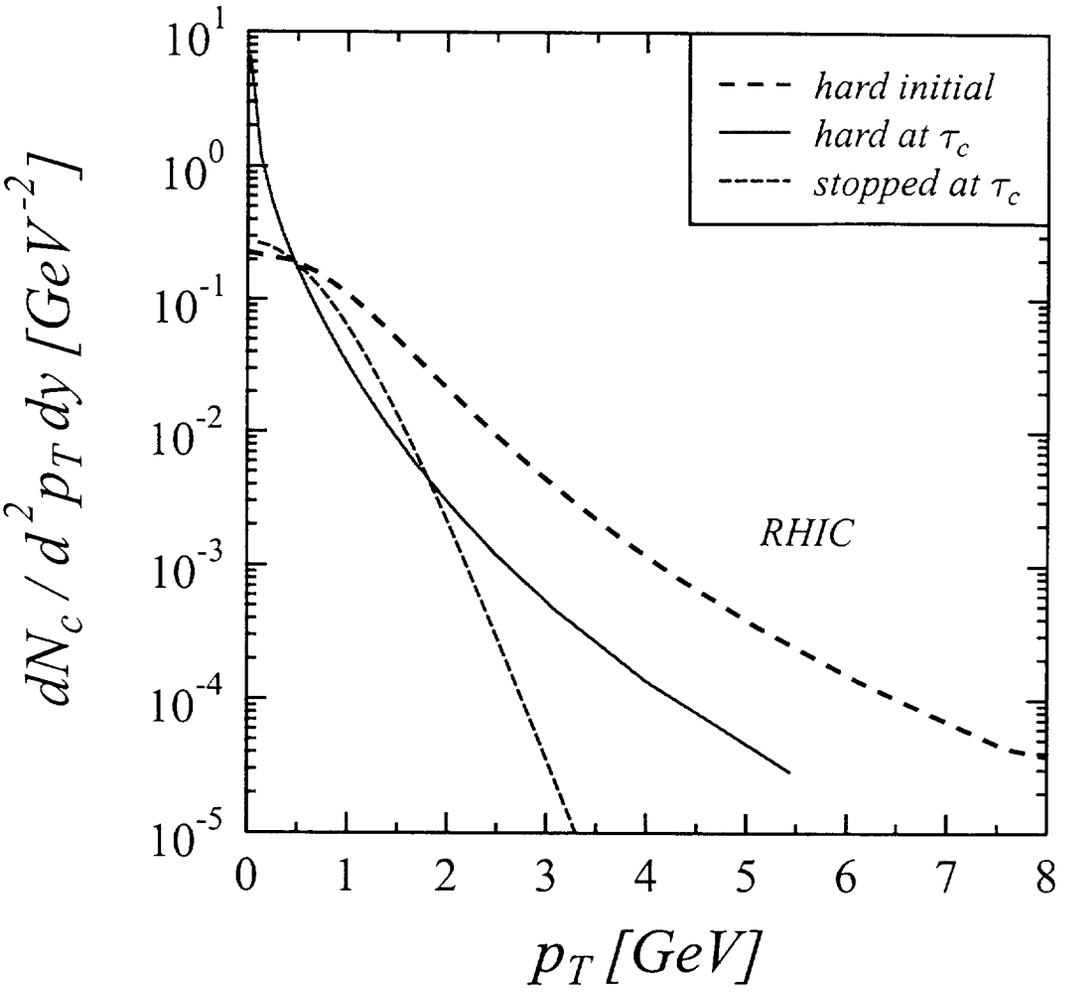

Figure 4. Transverse momentum spectrum of charm quarks. The fat-dashed curve depicts the initial spectrum [9], while the full line shows the spectrum (4) after momentum degradation. The short-dashed curve represents the thermalized part (5).

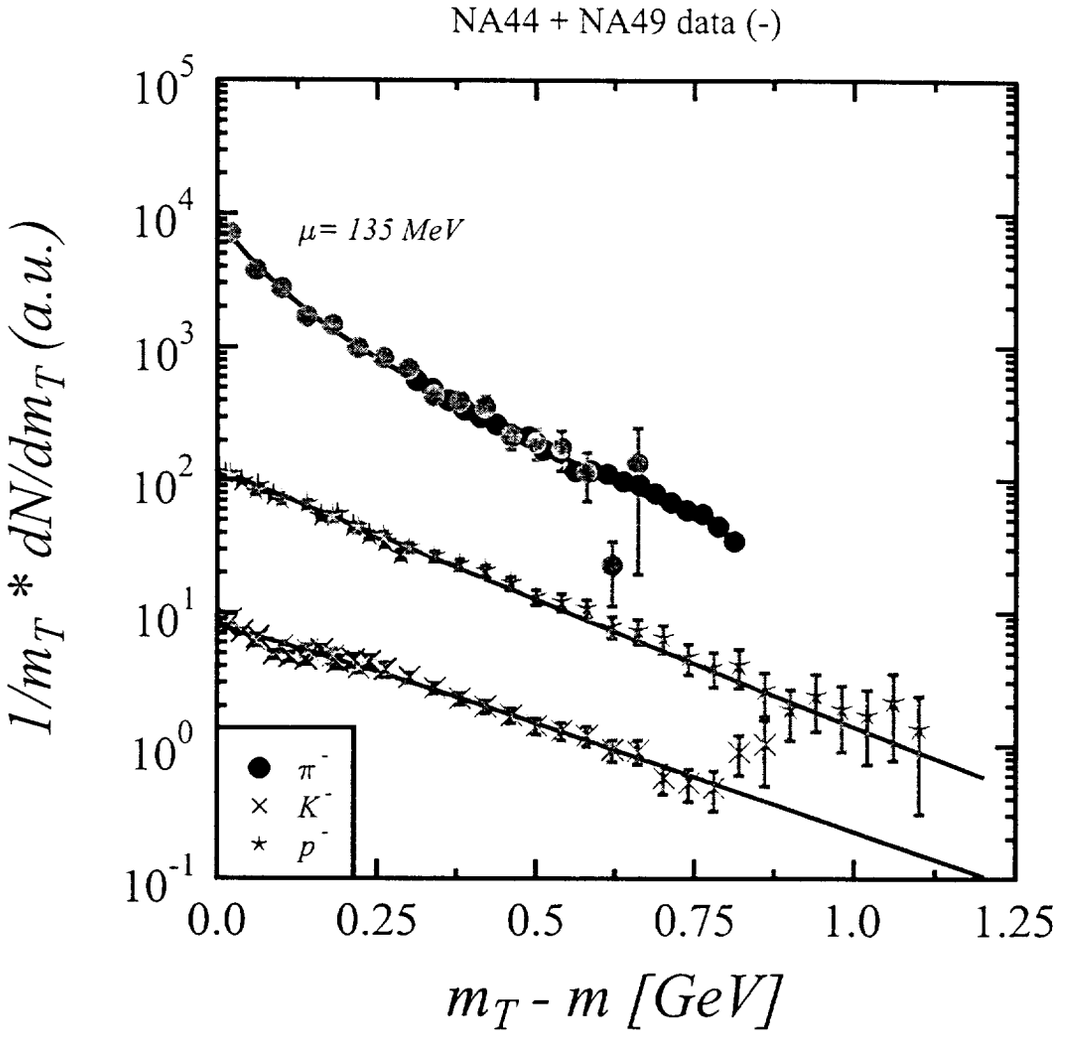

Figure 5. Fits of the transverse momentum spectra in Pb + Pb collisions at 158 AGeV. Preliminary NA49 data (black symbols) from [27], and NA44 data (grey symbols) from [29]; the deuteron data from NA49 are very preliminary.

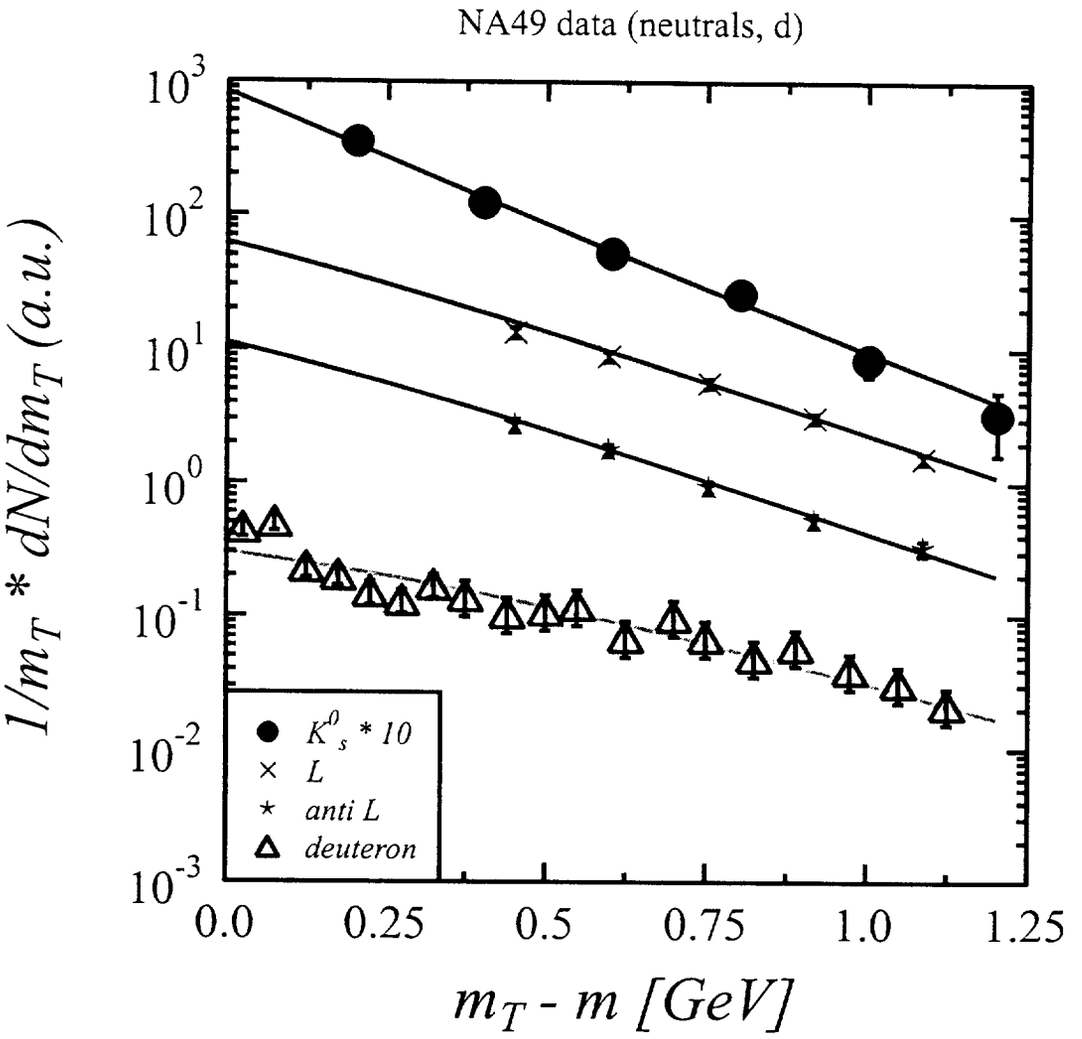

Figure 5. cont'd

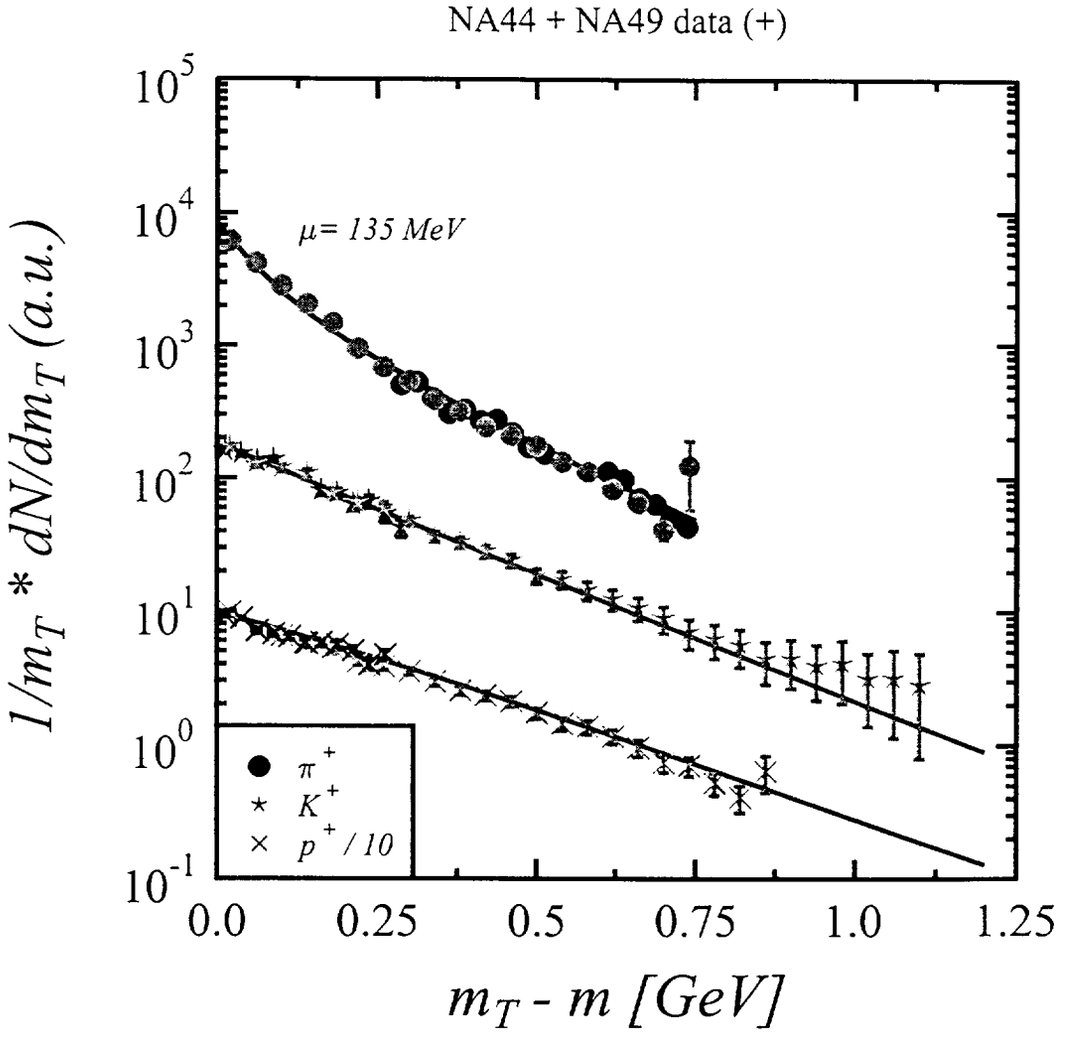

Figure 5. cont'd

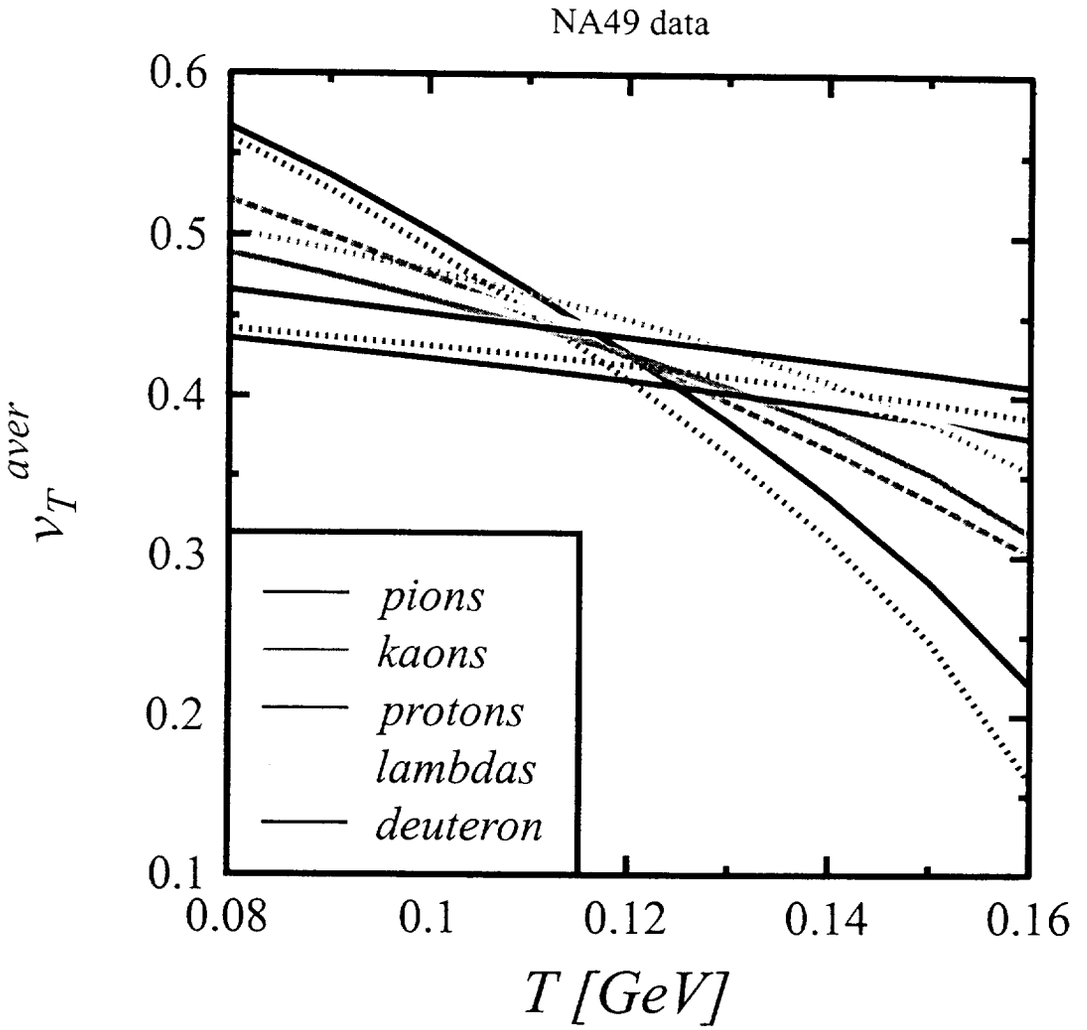

Figure 6. Individual fits of the NA49 data [27] with equation (5). Full, dashed, dotted lines are for negative, positive and neutral particle species.

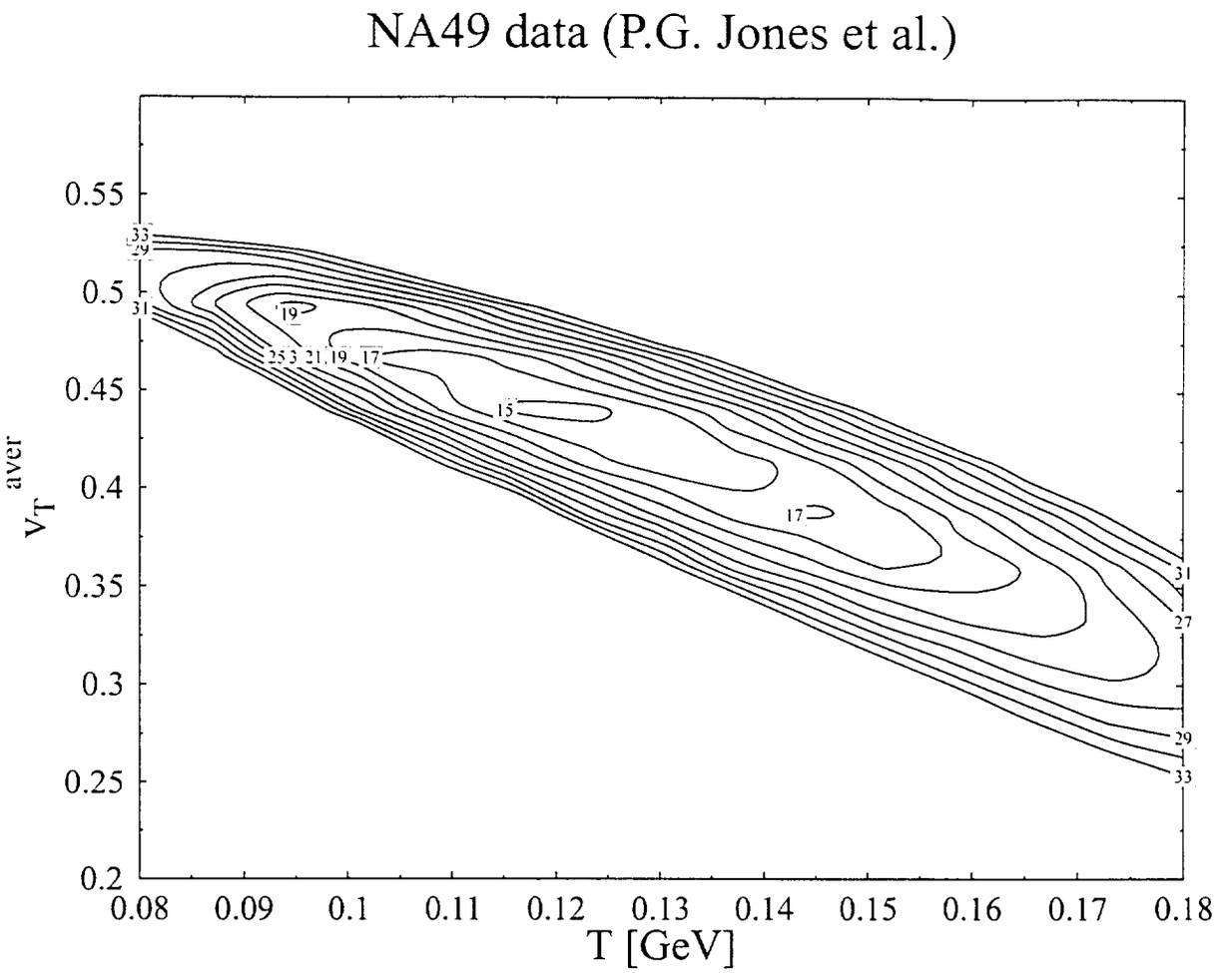

Figure 7. Contour plots of $\chi^2(T, v_\perp^{\rm aver})$ for the NA49 data [27].